PHOTONICS Research

Optomechanically induced transparency in a spinning resonator

Hao Lü,[1,2] Yajing Jiang,[3] Yu-Zhu Wang,[1] and Hui Jing[4,*]

[1]Key Laboratory for Quantum Optics, Shanghai Institute of Optics and Fine Mechanics, Chinese Academy of Sciences, Shanghai 201800, China
[2]University of Chinese Academy of Sciences, Beijing 100049, China
[3]Department of Physics, Henan Normal University, Xinxiang 453007, China
[4]Key Laboratory of Low-Dimensional Quantum Structures and Quantum Control of Ministry of Education, Department of Physics and Synergetic Innovation Center for Quantum Effects and Applications, Hunan Normal University, Changsha 410081, China
*Corresponding author: jinghui73@foxmail.com

Received 15 May 2017; revised 20 June 2017; accepted 20 June 2017; posted 21 June 2017 (Doc. ID 295823); published 21 July 2017

We study optomechanically induced transparency in a spinning microresonator. We find that in the presence of rotation-induced Sagnac frequency shift, both the transmission rate and the group delay of the signal are strongly affected, leading to a Fano-like spectrum of transparency. In particular, tuning the rotary speed leads to the emergence of nonreciprocal optical sidebands. This indicates a promising new way to control hybrid light–sound devices with spinning resonators.

OCIS codes: (270.1670) Coherent optical effects; (120.4880) Optomechanics.

https://doi.org/10.1364/PRJ.5.000367

1. INTRODUCTION

Cavity optomechanics (COM) research has progressed rapidly in recent years [1,2], leading to prospects and applications of nano-COM technologies, such as quantum state transducers [3–6], highly sensitive motion sensors [7,8], and coherent phonon lasing [9–11]. Few-photon-based COM has also been explored and is particularly useful for applications in COM-based quantum phononic engineering or quantum information processing [12–15]. Another example closely related to this work is the experimental demonstrations of optomechanically induced transparency (OMIT) [16–20]. Nonlinear OMIT effects and OMIT-based switching of slow to fast light have also been shown [19–25]. These advances indicate that versatile coherent control of light is achievable with solid-state COM devices.

In OMIT, radiation-pressure-induced breathing-mode oscillations of the boundary of the resonator play a key role, as in most COM devices. The possible role of the rotation of the resonator itself, however, has not been explored. In a rotating device, an additional phase is accumulated for the propagating light, known as the optical Sagnac effect [26,27]. Recently, exotic rotation-induced effects have been revealed in purely optical systems [28–33]. For example, the rotation-induced mode splitting in an optical microresonator, i.e., the frequency difference between the clockwise (CW) and the counterclockwise (CCW) modes, was revealed to provide a method for sensitive measurements of the angular velocity of the medium [28]; in addition, optical chiral symmetry breaking and other relevant effects have also been investigated [29–33]. In acoustics, we note that sound isolation was achieved in a recent experiment by using a circulating fluid medium [34].

Here we study the OMIT in a rotating microresonator. We show that both the transmission rate and the group delay of the probe can be flexibly tuned by steering the Sagnac shift. We find that the optical sidebands strongly depend on the rotary direction of the resonator, indicating a new scheme to achieve optical nonreciprocality, which is distinct from nonlinearity-based schemes as already demonstrated in recent experiments [35–39]. We stress that our work, using only a spinning resonator, is clearly different from a recent proposal: in Refs. [40,41], a COM system placed on a rotating table, including the cavity, the driving source, and the detectors, were considered to detect the Coriolis force or to turn off/on the OMIT, with a fixed rotary direction and also a cavity restricted along the diameter of the table. The main features of our work here, i.e., the optical nonreciprocality (transmitted or blocked) and the tunable group delay, by steering rotary directions of the resonator itself, were not revealed in all previous works. In addition, our work holds the promise to be extended to, e.g., a spinning nonlinear resonator, coupled spinning resonators, or a lattice of spinning resonators, to further steer the optical nonreciprocality, the slow light, and even topological COM effects [42,43].

2. THEORETICAL MODEL

As shown in Fig. 1, we consider a rotating whispering-gallery-mode (WGM) microresonator coupled to a stationary tapered fiber. This resonator, with optical resonance frequency ω_a and

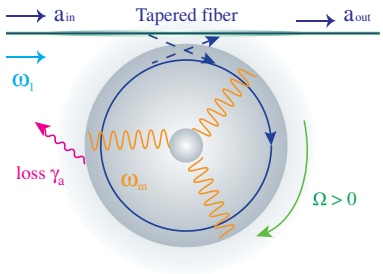

Fig. 1. Optomechanics in a rotating microresonator coupled to a stationary tapered fiber. The resonator contains a mechanical mode at frequency ω_m, driven by a pump field at frequency ω_l, and the frequency of rotation is positive ($\Omega > 0$) for the CW direction.

intrinsic loss $\gamma_a = \omega_a/Q$ (Q is the optical quality factor), is driven by a strong pump field at frequency ω_l and a weak probe at frequency ω_p. The amplitudes of the pump and probe fields are, respectively, $\varepsilon_l = \sqrt{P_l/\hbar\omega_l}$, and $\varepsilon_p = \sqrt{P_{\rm in}/\hbar\omega_p}$, where P_l or $P_{\rm in}$ denotes the pump or probe power, respectively. The resonator also contains a mechanical mode at frequency ω_m, driven by the pump field, and the frequency of rotation is denoted as Ω. Because the Sagnac effect, the frequency of the optical mode experiences a Sagnac–Fizeau shift [44], i.e.,

$$\omega_a \to \omega_a + \Delta_{\rm sag}, \tag{1}$$

$$\Delta_{\rm sag} = \frac{nr\Omega\omega_a}{c}\left(1 - \frac{1}{n^2} - \frac{\lambda}{n}\frac{{\rm d}n}{{\rm d}\lambda}\right), \tag{2}$$

where n or r is the refractive index or the radius of the resonator, respectively, c is the light speed in vacuum, and the dispersion term ${\rm d}n/{\rm d}\lambda$, characterizing the relativistic origin of the Sagnac effect, is relatively small in typical materials (~1%).

The Hamiltonian of the system, in a frame rotating at the pump frequency ω_l, can be written at the simplest level as ($\hbar = 1$)

$$\begin{aligned} H = {} & \Delta_+ a^\dagger a - \xi x a^\dagger a + \frac{p^2}{2m} + \frac{1}{2}m\omega_m^2 x^2 + \frac{p_\theta^2}{2mr^2} \\ & + i\sqrt{\gamma_{\rm ex}}\varepsilon_l(a^\dagger e^{-i\omega_l t} - a e^{i\omega_l t}) \\ & + i\sqrt{\gamma_{\rm ex}}\varepsilon_p(a^\dagger e^{-i\omega_p t} - a e^{i\omega_p t}), \end{aligned} \tag{3}$$

where $\Delta_+ = \Delta_a + \Delta_{\rm sag}$, $\Delta_a = \omega_a - \omega_l$, $\xi = \omega_a/r$ is the COM coupling, $\gamma_{\rm ex}$ is the loss due to the resonator–fiber coupling, a is the optical annihilation operator, and x, p, θ and p_θ denote the displacement, momentum, rotation angle, and angular momentum operators [41], respectively, with the commutation relations $[x, p] = [\theta, p_\theta] = i$. To compare with the familiar OMIT spectrum [16], here we ignore the Kerr effect of the materials, which, as demonstrated in a recent transient-OMIT experiment, can be compensated for by shifting the driving frequency, even for a strong driving [18]. Thermal effects can be further weakened in a similar way, besides using a cryostat device [16].

The Heisenberg equations of motion of the system are then written as

$$\begin{aligned} \dot{a} &= -(i\Delta_+ - i\xi x + \beta)a + \sqrt{\gamma_{\rm ex}}\varepsilon_l + \sqrt{\gamma_{\rm ex}}\varepsilon_p e^{-i\eta t}, \\ \ddot{x} + \gamma_m\dot{x} + \omega_m^2 x &= \frac{\xi}{m}a^\dagger a + \frac{p_\theta^2}{m^2 r^3}, \\ \dot{\theta} &= \frac{p_\theta}{mr^2}, \\ \dot{p}_\theta &= 0, \end{aligned} \tag{4}$$

where γ_m is the mechanical damping rate, $\eta = \omega_p - \omega_l$ is the frequency detuning between the probe and pump lights, and, for simplicity, the total optical loss is denoted as $\beta = (\gamma_a + \gamma_{\rm ex})/2$.

The steady-state values of the dynamical variables can be obtained as

$$\begin{aligned} \bar{a} &= \frac{\sqrt{\gamma_{\rm ex}}\varepsilon_l}{\beta + i\Delta_+ - i\xi\bar{x}}, \\ \bar{x} &= \frac{\gamma_{\rm ex}\xi|\varepsilon_l|^2}{m\omega_m^2[\beta^2 + (\Delta_+ - \xi\bar{x})^2]^2} + r\left(\frac{\Omega}{\omega_m}\right)^2, \end{aligned} \tag{5}$$

where $\Omega = \dot{\theta}$ is the speed of rotation. Clearly, besides the optical pump, the rotation also affects the values of both the mechanical displacement $\bar{x}$ and the intracavity optical amplitude $\bar{a}$. This means that the effective COM coupling or the breathing mode oscillations can be tuned by the rotation, which in turn results in modified OMIT properties of the system.

In order to see this, we use the standard procedure by expanding every operator as the sum of its steady value and a small fluctuation, i.e.,

$$\begin{aligned} a &= \bar{a} + \delta a_- e^{-i\eta t} + \delta a_+ e^{i\eta t}, \\ x &= \bar{x} + \delta x e^{-i\eta t} + \delta x^* e^{i\eta t}. \end{aligned} \tag{6}$$

By substituting Eq. (6) into Eq. (4), we have

$$\begin{aligned} &(\beta + i\Delta_+ - i\xi\bar{x} - i\eta)\delta a_- - i\xi\bar{a}\delta x = \sqrt{\gamma_{\rm ex}}\varepsilon_p, \\ &(\beta - i\Delta_+ + i\xi\bar{x} - i\eta)\delta a_+^* + i\xi\bar{a}^*\delta x = 0, \\ &(\omega_m^2 - \eta^2 - i\eta\gamma_m)\delta x = \frac{\xi}{m}(\bar{a}^*\delta a_- + \bar{a}\delta a_+^*). \end{aligned} \tag{7}$$

Solving these equations leads to

$$\delta a_- = \frac{\sqrt{\gamma_{\rm ex}}\varepsilon_p}{h_1(\eta)}\left[1 + \frac{i|\bar{a}|^2\xi^2\chi(\eta)}{h_1(\eta) - 2|\bar{a}|^2\xi^2\chi(\eta)h_2(\eta)}\right], \tag{8}$$

$$\begin{aligned} h_1(\eta) &= \beta + i\Delta_+ - i\xi\bar{x} - i\eta, \\ h_2(\eta) &= \frac{\Delta_+ - \xi\bar{x}}{\beta - i\Delta_+ + i\xi\bar{x} - i\eta}, \\ \chi(\eta) &= \frac{1}{m(\omega_m^2 - \eta^2 - i\gamma_m\eta)}. \end{aligned} \tag{9}$$

The expectation value of the output field can then be obtained by using the input–output relation, i.e.,

$$a_{\rm out} = a_{\rm in} - \sqrt{\gamma_{\rm ex}}\delta a_-, \tag{10}$$

where $a_{\rm in}$ and $a_{\rm out}$ are the input and output field operators, respectively, and the transmission rate of the probe field turns out to be

$$T = |t_p|^2 = \left|\frac{a_{\rm out}}{a_{\rm in}}\right|^2 = \left|1 - \frac{\sqrt{\gamma_{\rm ex}}}{\varepsilon_p}\delta a_-\right|^2. \tag{11}$$

This sets the stage for our discussion of the impact of rotation on the transmission rate and the group delay of the probe light.

3. RESULTS AND DISCUSSION

The transmission T is shown in Fig. 2 as a function of the detuning $\Delta_p \equiv \omega_p - \omega_a$ and the rotation speed, with experimentally feasible values [45], i.e., $n = 1.44$, $Q = 3 \times 10^7$, $r = 0.25$ mm, $\lambda = 1.55$ μm, $\gamma_{ex} = \gamma_a = \omega_a/Q$, $P_l = 10$ W, $\Delta_a = \omega_m$, $m = 2$ μg, $\omega_m = 200$ MHz, and $\gamma_m = 0.2$ MHz. For the familiar stationary case, the OMIT window appears around the resonance, $\Delta_p = 0$, due to destructive interference of the probe absorption. As shown in Ref. [16], the OMIT linewidth is approximately $\gamma_m + \xi^2|\tilde{a}|^2/\beta m^2\omega_m^2$; in the presence of rotation, the modified values of $\bar{x}$ and $\tilde{a}$ change the OMIT spectrum; see the red and blue curves in Fig. 2(a). Note that the rotation leads to a strong enhancement of $\xi\bar{x}$, resulting in redshifts of the OMIT peaks, i.e., from $\Delta_p = 0$ to $\Delta_p < 0$. Even at the resonance, significant differences emerge for different rotary directions. To clearly see this, we define the enhancement factor of transmission at the resonance

$$f = \frac{T(\Omega \neq 0)}{T(\Omega = 0)}\bigg|_{\Delta_p = 0} - 1. \tag{12}$$

Interestingly, as shown in Fig. 2(b), f increases with the rotation speed, but with different ratios for $\Omega > 0$ or $\Omega < 0$. For $\Omega = 120$ kHz, the transmission at $\Delta_p = 0$ is enhanced by ~11%. This holds the promise to be useful for practical applications of OMIT in coherent control of light.

For the stationary case, the OMIT peak appears at the resonance $\Delta_p = 0$, and for the off-resonance cases, a symmetric sideband dip appears on each side of the peak, indicating strong absorption of the off-resonance probe. Our scheme provides a new way to tune the positions of the OMIT peak and dips. In particular, for the off-resonance cases, the transmission rates of the probe depend on the rotary directions of the resonator (even transmitted or blocked for the input probe). This can be referred to as nonreciprocal optical sidebands (for other ways of tuning OMIT sidebands, see, e.g., Ref. [24]). For example, the frequency shift of the lower sideband is approximately $-\xi\bar{x} \mp |\Delta_{sag}|$, where $\mp$ corresponds to $\Omega > 0$ or $\Omega < 0$. In Figs. 2(c) and 2(d), we choose $\Omega = 100$ kHz and thus $\xi\bar{x} \approx 49$ MHz, and $|\Delta_{sag}| \approx 12$ MHz. In particular, $T(\Omega > 0) > 0.9$, while $T(\Omega < 0) \approx 0$ at $\Delta_p \approx -37$ MHz, i.e., featuring nonreciprocality in this situation. This indicates that, by tuning Ω and Δ_p, the probe light can be transmitted or blocked. Note that for a fixed rotary direction, $\Omega < 0$ corresponds to the case with the pump and probe lights applied from the right of the fiber. In this case, the probe coming from the left or the right can be transmitted or blocked. A similar feature was also observed in a purely optical experiment with a spinning resonator [46].

Accompanied with the OMIT, the slow light can also be observed [17]. This can be characterized by the group delay of the probe light:

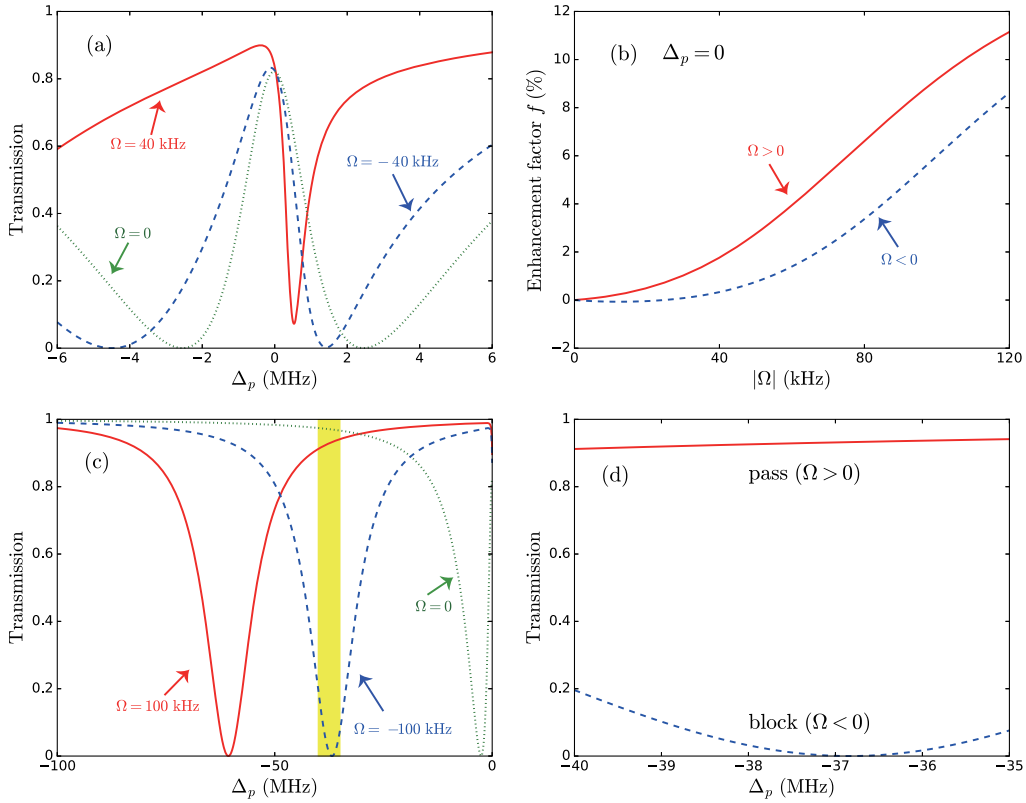

Fig. 2. (a, c, d) Transmission of the probe light as a function of the optical detuning Δ_p and (b) rotation speed $|\Omega|$. The rotation speed is set as (a, b) 40 kHz and (c, d) 100 kHz.

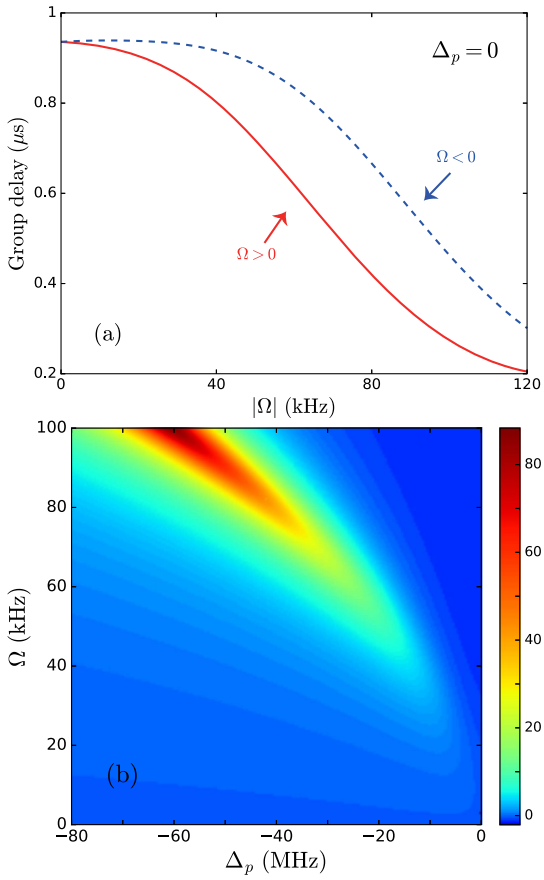

Fig. 3. (a) Group delay of the probe light τ_g at $\Delta_p = 0$, as a function of the rotation speed $|\Omega|$. (b) Enhancement factor of the group delay D as a function of the probe detuning Δ_p and rotation speed $|\Omega|$.

$$\tau_g = \frac{\mathrm{d}\arg(t_p)}{\mathrm{d}\Delta_p}. \tag{13}$$

As shown in Fig. 3, τ_g now depends on both Ω and Δ_p. For $\Delta_p = 0$, the probe light tends to pass with a higher transmission [Fig. 2(b)] but also with a higher velocity [Fig. 3(a)], highlighting different roles of OMIT and the Sagnac effect; for $\Delta_p \neq 0$, we define the enhancement factor of group delay:

$$D = \frac{\tau_g(\Omega \neq 0)}{\tau_g(\Omega = 0)} - 1. \tag{14}$$

Figure 3(b) shows D as a function of Ω and Δ_p. Clearly, to achieve both a higher transmission and a higher group delay, one needs to carefully choose the values of Ω and Δ_p. For example, for $\Omega = 100$ kHz and $\Delta_p = -75$ MHz, we have $D \approx 22$ and $T \approx 0.85$, indicating the possibility of achieving enhanced slow light with a still considerable transmission rate. In comparison with conventional COM devices, our spinning-OMIT scheme provides a new degree of freedom to adjust the properties of optical propagations.

4. CONCLUSION

In summary, we have studied OMIT in a spinning resonator. We find that the mechanical oscillation and the intracavity photons are strongly affected by the rotation-induced Sagnac effect, which in turn leads to significantly modified OMIT properties, including the transmission rate and the group delay of the probe. In particular, the optical sidebands, depending on the directions of rotation, exhibit a highly asymmetric feature (i.e., transmitted or blocked for incoming signals from left or right). We note that the Sagnac effect can be applied to induce different shifts for the forward and backward signals in Brillouin-scattering-induced transparency [47], in which the nonreciprocal light propagation may be more easily observed with a lower rotation speed.

The rotation of the resonator is now up to ~100 kHz, i.e., still far less than the mechanical frequency. We expect that by further enhancing the rotation speed, new effects such as optical chaotic dynamics or other interesting effects (even rotational–vibrational coupling) [48,49] may be detected, which, however, need to be explored in future work. We believe that spinning devices hold the promise to find applications in a wide range of COM-based applications such as optical isolating [35] or chiral sensing [50].

Funding. National Natural Science Foundation of China (NSFC) (11474087, 91536107); Key Research Program of Frontier Science of Chinese Academy of Sciences (CAS) (QYZDY-SSW-SLH009); National Key R&D Program of China (2016YFA0301504).

Acknowledgment. Insightful discussions with Shai Maayani, Tal Carmon, and Chun-Hua Dong are acknowledged.

REFERENCES

1. M. Aspelmeyer, T. J. Kippenberg, and F. Marquardt, "Cavity optomechanics," Rev. Mod. Phys. **86**, 1391–1452 (2014).
2. M. Metcalfe, "Applications of cavity optomechanics," Appl. Phys. Rev. **1**, 031105 (2014).
3. T. Bagci, A. Simonsen, S. Schmid, L. G. Villanueva, E. Zeuthen, J. Appel, J. M. Taylor, A. Sørensen, K. Usami, A. Schliesser, and E. S. Polzik, "Optical detection of radio waves through a nanomechanical transducer," Nature **507**, 81–85 (2014).
4. F. Lecocq, J. B. Clark, R. W. Simmonds, J. Aumentado, and J. D. Teufel, "Mechanically mediated microwave frequency conversion in the quantum regime," Phys. Rev. Lett. **116**, 043601 (2016).
5. X.-W. Xu, Y. Li, A.-X. Chen, and Y.-X. Liu, "Nonreciprocal conversion between microwave and optical photons in electro-optomechanical systems," Phys. Rev. A **93**, 023827 (2016).
6. T.-Y. Chen, W.-Z. Zhang, R.-Z. Fang, C.-Z. Hang, and L. Zhou, "Multi-path photon-phonon converter in optomechanical system at single-quantum level," Opt. Express **25**, 10779–10790 (2017).
7. O. Arcizet, P.-F. Cohadon, T. Briant, M. Pinard, A. Heidmann, J.-M. Mackowski, C. Michel, L. Pinard, O. Franais, and L. Rousseau, "High-sensitivity optical monitoring of a micromechanical resonator with a quantum-limited optomechanical sensor," Phys. Rev. Lett. **97**, 133601 (2006).
8. E. Gavartin, P. Verlot, and T. J. Kippenberg, "A hybrid on-chip optomechanical transducer for ultrasensitive force measurements," Nat. Nanotechnol. **7**, 509–514 (2012).
9. I. S. Grudinin, H. Lee, O. Painter, and K. J. Vahala, "Phonon laser action in a tunable two-level system," Phys. Rev. Lett. **104**, 083901 (2010).
10. H. Jing, S. K. Özdemir, X.-Y. Lü, J. Zhang, L. Yang, and F. Nori, "PT-symmetric phonon laser," Phys. Rev. Lett. **113**, 053604 (2014).
11. G. Wang, M. Zhao, Y. Qin, Z. Yin, X. Jiang, and M. Xiao, "Demonstration of an ultra-low-threshold phonon laser with coupled microtoroid resonators in vacuum," Photon. Res. **5**, 73–76 (2017).

12. A. Nunnenkamp, K. Brkje, and S. M. Girvin, "Single-photon optomechanics," Phys. Rev. Lett. **107**, 063602 (2011).
13. I. M. Mirza and S. J. van Enk, "Single-photon time-dependent spectra in quantum optomechanics," Phys. Rev. A **90**, 043831 (2014).
14. J.-Q. Liao and C. K. Law, "Correlated two-photon scattering in cavity optomechanics," Phys. Rev. A **87**, 043809 (2013).
15. I. M. Mirza, "Strong coupling optical spectra in dipole–dipole interacting optomechanical Tavis–Cummings models," Opt. Lett. **41**, 2422–2425 (2016).
16. S. Weis, R. Rivière, S. Deléglise, E. Gavartin, O. Arcizet, A. Schliesser, and T. J. Kippenberg, "Optomechanically induced transparency," Science **330**, 1520–1523 (2010).
17. A. H. Safavi-Naeini, T. P. Mayer Alegre, J. Chan, M. Eichenfield, M. Winger, Q. Lin, J. T. Hill, D. E. Chang, and O. Painter, "Electromagnetically induced transparency and slow light with optomechanics," Nature **472**, 69–73 (2011).
18. Z. Shen, C.-H. Dong, Y. Chen, Y.-F. Xiao, F.-W. Sun, and G.-C. Guo, "Compensation of the Kerr effect for transient optomechanically induced transparency in a silica microsphere," Opt. Lett. **41**, 1249–1252 (2016).
19. X. Zhou, F. Hocke, A. Schliesser, A. Marx, H. Huebl, R. Gross, and T. J. Kippenberg, "Slowing, advancing and switching of microwave signals using circuit nanoelectromechanics," Nat. Phys. **9**, 179–184 (2013).
20. M. Asano, Ş. K. Özdemir, W. Chen, R. Ikuta, L. Yang, N. Imoto, and T. Yamamoto, "Controlling slow and fast light and dynamic pulse-splitting with tunable optical gain in a whispering-gallery-mode microcavity," Appl. Phys. Lett. **108**, 181105 (2016).
21. H. Jing, Ş. K. Özdemir, Z. Geng, J. Zhang, X.-Y. Lü, B. Peng, L. Yang, and F. Nori, "Optomechanically-induced transparency in parity-time-symmetric microresonators," Sci. Rep. **5**, 9663 (2015).
22. A. Kronwald and F. Marquardt, "Optomechanically induced transparency in the nonlinear quantum regime," Phys. Rev. Lett. **111**, 133601 (2013).
23. L. Fan, K. Y. Fong, M. Poot, and H. X. Tang, "Cascaded optical transparency in multimode-cavity optomechanical systems," Nat. Commun. **6**, 5850 (2015).
24. H. Xiong, L.-G. Si, A.-S. Zheng, X. Yang, and Y. Wu, "Higher-order sidebands in optomechanically induced transparency," Phys. Rev. A **86**, 013815 (2012).
25. Y. Jiao, H. Lü, J. Qian, Y. Li, and H. Jing, "Nonlinear optomechanics with gain and loss: amplifying higher-order sideband and group delay," New J. Phys. **18**, 083034 (2016).
26. E. J. Post, "Sagnac effect," Rev. Mod. Phys. **39**, 475–493 (1967).
27. W. W. Chow, J. Gea-Banacloche, L. M. Pedrotti, V. E. Sanders, W. Schleich, and M. O. Scully, "The ring laser gyro," Rev. Mod. Phys. **57**, 61–104 (1985).
28. C. Ciminelli, F. Dell'Olio, C. E. Campanella, and M. N. Armenise, "Photonic technologies for angular velocity sensing," Adv. Opt. Photon. **2**, 370–404 (2010).
29. L. Ge, R. Sarma, and H. Cao, "Rotation-induced mode coupling in open wavelength-scale microcavities," Phys. Rev. A **90**, 013809 (2014).
30. R. Sarma, L. Ge, J. Wiersig, and H. Cao, "Rotating optical microcavities with broken chiral symmetry," Phys. Rev. Lett. **114**, 053903 (2015).
31. M. P. J. Lavery, F. C. Speirits, S. M. Barnett, and M. J. Padgett, "Detection of a spinning object using light's orbital angular momentum," Science **341**, 537–540 (2013).
32. G. Li, T. Zentgraf, and S. Zhang, "Rotational Doppler effect in nonlinear optics," Nat. Phys. **12**, 736–740 (2016).
33. S. Franke-Arnold, G. Gibson, R. W. Boyd, and M. J. Padgett, "Rotary photon drag enhanced by a slow-light medium," Science **333**, 65–67 (2011).
34. R. Fleury, D. L. Sounas, C. F. Sieck, M. R. Haberman, and A. Alù, "Sound isolation and giant linear nonreciprocity in a compact acoustic circulator," Science **343**, 516–519 (2014).
35. Z. Shen, Y.-L. Zhang, Y. Chen, C.-L. Zou, Y.-F. Xiao, X.-B. Zou, F.-W. Sun, G.-C. Guo, and C.-H. Dong, "Experimental realization of optomechanically induced non-reciprocity," Nat. Photonics **10**, 657–661 (2016).
36. F. Ruesink, M.-A. Miri, A. Alù, and E. Verhagen, "Nonreciprocity and magnetic-free isolation based on optomechanical interactions," Nat. Commun. **7**, 13662 (2016).
37. K. Fang, J. Luo, A. Metelmann, M. H. Matheny, F. Marquardt, A. A. Clerk, and O. Painter, "Generalized non-reciprocity in an optomechanical circuit via synthetic magnetism and reservoir engineering," Nat. Phys. **13**, 465–471 (2017).
38. Q.-T. Cao, H. Wang, C.-H. Dong, H. Jing, R.-S. Liu, X. Chen, L. Ge, Q. Gong, and Y.-F. Xiao, "Experimental demonstration of spontaneous chirality in a nonlinear microresonator," Phys. Rev. Lett. **118**, 033901 (2017).
39. M. Scheucher, A. Hilico, E. Will, J. Volz, and A. Rauschenbeutel, "Quantum optical circulator controlled by a single chirally coupled atom," Science **354**, 1577–1580 (2016).
40. S. Davuluri and Y. V. Rostovtsev, "Quantum optical mouse to detect Coriolis force," Europhys. Lett. **103**, 24001 (2013).
41. S. Davuluri and S. Zhu, "Controlling optomechanically induced transparency through rotation," Europhys. Lett. **112**, 64002 (2015).
42. H. Xu, D. Mason, L. Jiang, and J. G. E. Harris, "Topological energy transfer in an optomechanical system with exceptional points," Nature **537**, 80–83 (2016).
43. H. Jing, Ş. K. Özdemir, H. Lü, and F. Nori, "High-order exceptional points in optomechanics," Sci. Rep. **7**, 3386 (2017).
44. G. B. Malykin, "The Sagnac effect: correct and incorrect explanations," Phys. Usp. **43**, 1229–1252 (2000).
45. H. Guo, M. Karpov, E. Lucas, A. Kordts, M. H. P. Pfeiffer, V. Brasch, G. Lihachev, V. E. Lobanov, M. L. Gorodetsky, and T. J. Kippenberg, "Universal dynamics and deterministic switching of dissipative Kerr solitons in optical microresonators," Nat. Phys. **13**, 94–102 (2017).
46. S. Maayani and T. Carmon (personal communication).
47. C.-H. Dong, Z. Shen, C.-L. Zou, Y.-L. Zhang, W. Fu, and G.-C. Guo, "Brillouin-scattering-induced transparency and non-reciprocal light storage," Nat. Commun. **6**, 6193 (2015).
48. W. M. Zhang and G. Meng, "Stability, bifurcation and chaos analyses of a high-speed micro-rotor system with rub-impact," Sens. Actuators A **127**, 163–178 (2006).
49. R. Kurose and S. Komori, "Drag and lift forces on a rotating sphere in a linear shear flow," J. Fluid Mech. **384**, 183–206 (1999).
50. D. Sofikitis, L. Bougas, G. E. Katsoprinakis, A. K. Spiliotis, B. Loppinet, and T. P. Rakitzis, "Evanescent-wave and ambient chiral sensing by signal-reversing cavity ringdown polarimetry," Nature **514**, 76–79 (2014).